IOSR Journal of Mathematics (IOSR-JM)
e-ISSN: 2278-5728, p-ISSN: 2319-765X. Volume 13, Issue 6 Ver. III (Nov. - Dec. 2017), PP 08-17
www.iosrjournals.org

Comparative Study of Netonian Sinusoidal Blood Flow through Normal and Stenosed Carotid Artery

Mohammad Matiur Rahman[1,a)],Md. Anwar Hossain[1,b)] ,
Khairuzzaman Mamun[1,c)] ,Most. Nasrin Akhter[1,d)].
[1](*Department of Mathematics, Dhaka University of Engineering and Technology, Gazipur-1700, Bangladesh)*
a)Corresponding author: matiurrahman1975@gmail.com
b) anwarmath23@gmail.com,c) presidentmamun@gmail.com,d) nasrin6092002@yahoo.com

Abstract: *A numerical simulation is performed to investigate Newtonian sinusoidal flows behavior on three dimensional idealized carotid artery (CA) and single stenosed (75% by area) carotid artery(SCA). The wall vessel is set as rigid during simulation. Bifurcated blood vessel are simulated by using three-dimensional flow analysis. Sinusoidal and parabolic velocity profiles are set out to fix the conditions of inlet boundaries of artery. The investigation has a Reynolds number range of 90 to 1430. Low Reynolds number* $k-\omega$ *model has been used as governing equation. The investigation has been carried out to characterize the flow behavior of blood in two geometry, namely, (i) Normal carotid artery (CA) and (ii) Stenosed carotid artery (SCA). The Newtonian model has been used to study the physics of fluid. The findings of the two models are thoroughly compared in order to observe there behavioral sequence of flows. The numerical results were presented in terms of velocity, pressure, wall shear stress distributions and cross sectional velocities as well as the streamlines contour. Stenosis disturbs the normal pattern of blood flow through the artery as reduced area. At stenosis region velocity and peak Reynolds number rapidly increase and Reynolds number reach transitional and turbulent region. These flow fluctuation and turbulence have bad effect to the blood vessel which makes to accelerate the progress of stenosis.*

Keywords : *Atherosclerosis, Carotid artery, Sinusoidal blood flow, Stenosis, Viscosity.*

Date of Submission: 15-11-2017 Date of acceptance: 30-11-2017

I. Introduction

Stroke is a prevalent and severe medical condition that imposes an immense loss of health and heavy economic burden worldwide. Globally, stroke is the second leading cause of death and the leading cause of long-term disability [1, 2]. The adverse effects are both extensive and long-lasting, as one third of new strokes result in death and most stroke survivors are afflicted by a neurological disability that requires rehabilitation or long-term care [3]. Moreover, once a stroke has occurred, the risk of stroke recurrence increases substantially [4, 5]. By far, the most common form of stroke is due to ischemia – a restriction or shortage in cerebral blood supply – which accounts for 78% of strokes [6]. Ischemia is most often caused by a thrombus or clot that has emblazed and travelled to the brain causing arterial occlusion of a narrow cerebral vessel [7, 10] The thrombus typically originates from a proximal location in the body, such as the heart (cardiogenic embolism) or from 2 atherosclerotic plaque in a large proximal artery (artery-to-artery embolism), commonly the aorta or internal carotid artery (ICA). Atherosclerosis localized in the carotid arteries is not only prevalent, but also represents a significant risk for clinical cerebrovascular events. The carotid artery is the most frequently involved site in large artery atherothrombotic stroke. Carotid artery atherothrombosis is estimated to be responsible for 10 – 30% of all strokes [4, 6-8]. the geometry of the flow vessel is a key determinant of its flow characteristics. It has been well established that stenoses, bifurcations, and surface roughness are associated with flow disturbances and complex flow [9-11].The influence of vessel geometry on flow is exemplified in the arterial vasculature. Even in the normal, healthy vasculature, vessel bends and bifurcations, as well as the pulsatile flow of the cardiac cycle, introduce secondary flows and oscillating shear stresses. Atherosclerosis admits yet more complications, particularly where arterial disease is severe enough to cause a vessel stenosis [15]. Whereas flow in normal arteries is complex but typically laminar, stenosis are associated with shear layers, eddy formation, distal flow disturbances [15], and velocity fluctuations [16]. Tortuous, irregular vessel surfaces are likely to further contribute to flow disturbances [9, 10]. At the stenosed carotid artery, flow first encounters an asymmetric bifurcating junction, then immediately goes through a stenotic flow constriction, followed downstream by a sudden expansion into the carotid bulb. The bifurcation imposes a flow division that affects the boundary layers along both the inside and outside bends, which is dependent on the exact branch geometry.

The comparison of stenosed flow behavior with the normal one can provide the proper understanding of underlying mechanism behind the development of atherosclerosis. The flow turns to be abnormal in the reduced cross sectional area of the artery stated by Kader and Shenory [7]. The flow behavior in the stenosed artery is quite different in comparison to the normal one. Stress and resistance to flow is much higher in stenosed artery. Chua and Shread [9] found that the flow through the constricted tube is characterized by high velocity jet generated at constricted region. Kader and Shenory [7] found the results from numerical simulation which demonstrated that velocity and stenotic jet length increases in increasing the severity of stenosis. Their results also demonstrate that the 3D stenotic CFD model is capable of predicting the changes in flow behavior for increased severity of stenosis. Young et al. [17] studied the wall shear stress and pressure gradient in the stenosis and evaluated the cause of plaque rupture. The authors studied pulsatile blood flow through the stenosis with elastic wall to observe the lumen movement. According to their study the peak WSS occurred just before minimum lumen position. Pinto et al. [18] performed numerical simulation assuming a physiological pulsatile flow through different models of stenosis. In case of subject-specific anatomically realistic stenosed carotid bifurcation subjected to pulsatile inlet condition, the simulation results demonstrated the rapid fluctuation of velocity and pressure in post-stenotic region by S. Lee and S. Lee [16]. Ahmed and Giddens [19] studied both steady and pulsatile flow through 25%, 50% and 75% constriction of a rigid tube where Reynolds number ranged from 500 to 2000. In another study, the stenosis having different geometric profiles like trapezium, semi-ellipse and triangle were analyzed considering the Non-Newtonian behavior by Lorenzini and Casalena [20]. Most of the researcher considered stenosed carotid artery or normal one. But in this study we use normal and stenosed carotid artery together to understand the flow behavior correctly. The investigation has a Reynolds number range of 90 to 1430. The numerical results are presented in terms of velocity, pressure, wall shear stress distributions.This paper is organized as follows. In section "Model description" we discuss the geometry and blood properties. In section " Governing equation and Numerical method we discuss the governing equation, boundary condition, grid independence check, validation and numerical scheme. In section "Results and discussion" we discuss and summaries the wss, velocity and pressure distributions through the carotid artery.

II. Model description

2.1 Geometry

Three dimensional carotid artery (CA) and 75% stenosed(by area) carotid artery (SCA) are used as geometry for this study shown in Fig. 1 (a). Bifurcation angles ICA $\left(29.5^0\right)$ and ECA $\left(18.5^0\right)$; the radius of the blood vessel CCA(4mm) , middle of stenosis (2mm), end of ICA(2.5mm), end of ECA(2mm); length of the artery from VI(i) are at position (j) 72mm, (k) 80mm, (l) 88mm, (m) and (n) 103mm, (o)and (p) 118mm and (q) and (r) 142mm; percent of stenosis (75% by area). Fig. 1(b) shows the mesh in cross-sectional plane of a carotid artery.

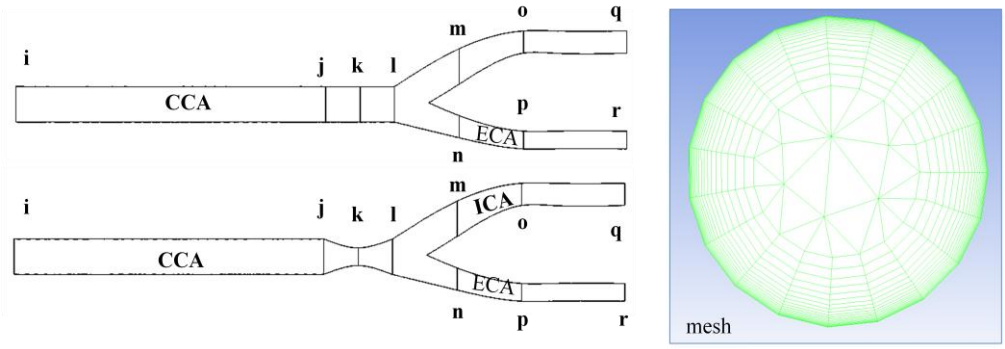

(a) (b)

Figure 1: (a) Model of a carotid artery ; (b) mesh in cross sectional plane of a carotid artery.

2.2 Blood properties

The density of the blood is 1050kg/m^3. In a Newtonian model for the blood viscosity, the value of μ is treated as a constant usually set to $\mu = 3.45 \times 10^{-3}\ pa.s$.

III. Governing Equation And Numerical Method

3.1 Governing equation

Due to constriction, blood passes through the throat and post stenotic region with high velocity. Flow velocity at post stenotic region increases but pressure of that region decreases. So, moderate and severe arterial stenosis restricts the flow severely with creating turbulent flow characteristics. For this region, turbulent flow is expected at post stenotic region especially for 75% stenotic artery. Neither laminar flow modeling nor standard two-equation models are suitable for this kind of blood flow. So, Wilcox low-Re turbulence model is more acceptable for flow analysis found by Varghese and Frankel [22]. Therefore, low Re $k-\omega$ turbulent model is taken for calculation.

Now, the Navier-Stokes equation can be given by-

$$\frac{\partial u_i}{\partial x_i} = 0 \tag{1}$$

$$\frac{\partial u_i}{\partial t} + u_j \frac{\partial u_i}{\partial x_j} = -\frac{1}{\rho}\frac{\partial p}{\partial x_i} + \frac{\partial^2 u_i}{\partial x_j \partial x_i} \tag{2}$$

Since each term of this equation is time averaged, the equation is referred to as a Reynolds averaged Navier-Stokes (RANS) equation. During this procedure, several additional unknown parameters appear which require additional equations to be introduced as turbulence models. The set of RANS equations are-

$$\frac{\partial \rho}{\partial t} + \frac{\partial (\rho u_i)}{\partial x} = 0 \tag{3}$$

$$\frac{\partial (\rho u_i)}{\partial t} + \frac{\partial (\rho u_i u_j)}{\partial x_j} = -\frac{\partial p}{\partial x_i} + \frac{\partial}{\partial x_j}\left[\mu\left(\frac{\partial u_i}{\partial x_j} + \frac{\partial u_j}{\partial x_i} - \frac{2}{3}\delta_{ij}\left(\frac{\partial u_1}{\partial x_1}\right)\right)\right] + \frac{\partial}{\partial t}\left(-\rho\overline{u_i' u_j'}\right) \tag{4}$$

In this equation $-\rho\overline{u_i' u_j'}$ is an additional term known as the Reynolds's stress tensor, which can be approximated by using Boussinesq's hypothesis-

$$-\rho\overline{u_i' u_j'} = \mu_t\left(\frac{\partial u_i}{\partial x_j} + \frac{\partial u_j}{\partial x_i}\right) - \frac{2}{3}\left(\rho k + \mu_t \frac{\partial u_k}{\partial x_k}\right) \tag{5}$$

Eddy viscosity can be modeled as a function of the turbulence kinetic energy (k) and specific dissipation rate (ω); therefore it is referred to as the two-equation turbulent model.

The turbulence kinetic energy **k** and specific dissipation rate **ω** of standard $k-\omega$ model are determined by following two equations:

The k equation: $$\frac{\partial}{\partial t}(\rho k) + \frac{\partial}{\partial x_i}(\rho k u_i) = \frac{\partial}{\partial x_j}\left(\Gamma_k \frac{\partial k}{\partial x_i}\right) + G_k - Y_k + S_k \tag{6}$$

The ω equation: $$\frac{\partial}{\partial t}(\rho \omega) + \frac{\partial}{\partial x_i}(\rho \omega u_i) = \frac{\partial}{\partial x_j}\left(\Gamma_\omega \frac{\partial \omega}{\partial x_i}\right) + G_\omega - Y_\omega + S_\omega \tag{7}$$

In these equations, G_k represents the generation of turbulence kinetic energy due to mean velocity gradients. G_ω represents the generation of ω. Γ_k and Γ_ω represent the effective diffusivity of k and ω, respectively. Y_k and Y_ω represent the dissipation of k and ω due to turbulence. S_k and S_ω are user-defined source terms.

A low Reynolds number correction factor controls the influence on the overall structure of the flow field, depending upon local conditions, and it is given as-

$$\alpha^* = \alpha_\infty^* \left(\frac{\alpha_0^* + \mathrm{Re}_t / R_k}{1 + \mathrm{Re}_t / R_k} \right) \tag{8}$$

Where, $\mathrm{Re}_t = \frac{\rho k}{\mu \omega}, R_k = 8, \alpha_0^* = \frac{\beta_i}{4}, \beta_i = 0.072, \alpha_\infty^* = 1.$

Closure Coefficient for the Transitional $k-\omega$ Model are-

$$\alpha_\infty^* = 1, \alpha_\infty = 0.52, \alpha_0 0.1111, \beta_\infty^* = 0.09, \beta_i = 0.072, R_k = 8 \, and \, R_\beta = 8$$

Detailed descriptions of sixteen harmonic coefficients are shown in TABLE 1. Here, Reynolds number varies from 90 to 1430. Since cardiac pulse cycle is 0.82sec, ω is pulsation, found from the calculation $\omega = \frac{2\pi}{0.82} = 7.66 \, rad/\sec$. Fig. 2(a) and 2(b) show oscillatory physiological waveform and parabolic inlet velocity profile respectively. In figure 2(a), a, b, and c represent the positions of early systole (0.0615sec), peak systole (0.1804 sec), and diastole (0.533 sec) respectively.

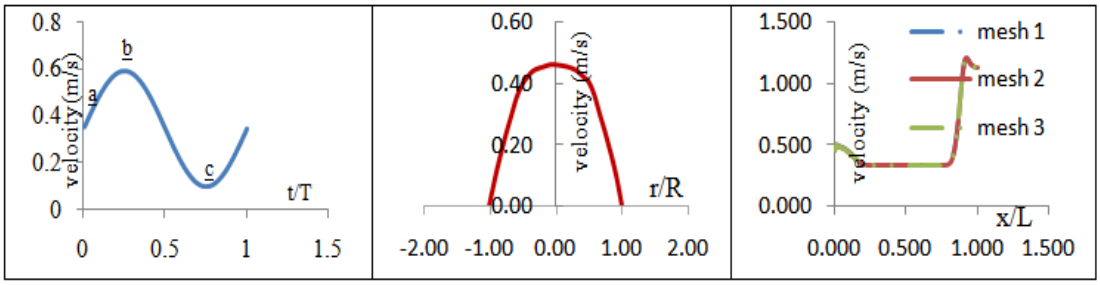

(a) (b) (c)

Figure 2: (a) oscillatory sinusoidal waveform, (b) parabolic inlet velocity profile, and (c) velocity distribution in 75% stenotic artery from different mesh sizes.

3.2 Grid independence check

An extensive test is carried out with different sizes of mesh such as mesh 1 (182030 element), mesh2 (230944 element) and mesh3 (279699 element) respectively. Fig 2(c) shows the velocity distributions for 75% stenosed carotid artery with mentioned mesh sizes. In all cases, the velocity distributions are same. It implies that the solution is grid independence.

3.3 Validation

Before starting of present investigation the numerical simulation is needed to be validated. Validation of the present numerical computation is done by plotting the steady velocity profile at downstream from the stenosis throat and comparing it with the velocity profile of Varghese and Frankel [22]. For this case, a parabolic velocity profile is assumed as inlet boundary condition. The mean inlet velocity corresponds to Reynolds number 500 and the flow is assumed to be steady. The results are shown in the Figure 3, where a good agreement can be found with Varghese and Frankel [22].

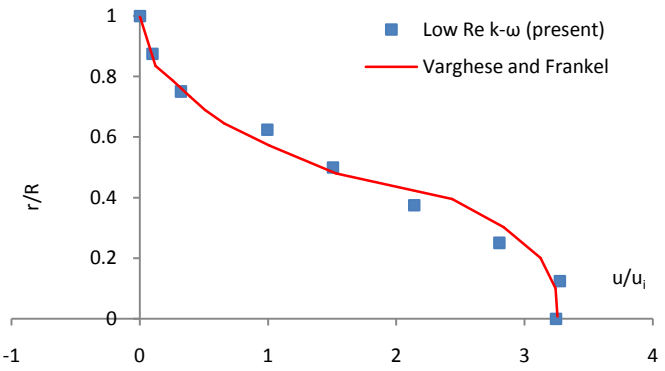

Figure 3: Validation with the velocity profile of Varghese and Frankel [22].

3.4 Numerical scheme

The numerical simulations are performed by well-known software ANSYS Fluent 14.5. A pressure based algorithm is chosen as the solver type. This solver is generally selected for an incompressible fluid. As there is no heat transfer in the blood flow process, energy equation is not solved. Since turbulent is expected in 75% stenotic carotid artery at post stenotic and bifurcation region, a low Reynolds number $k-\omega$ turbulent model is used throughout the work. In solution methods, the SIMPLE algorithm is selected for pressure-velocity coupling. First Order Upwind scheme is employed as a numerical scheme for discretization of the momentum equation. The time step is set to 0.00041 sec with 2000 number of total time steps. Maximum 10 iterations are performed per each time step.

IV. Results And Discussion Of Sinusoidal Blood Flow

The computational results of sinusoidal blood flow are conducted to study the influence of stenosis on the flow behavior. The flow parameters like velocity, pressure, WSS are observed from transverse and longitudinal contours at specific instants of pulse cycle for comparing the flow variation. The discussion is categorized with the observations of flow variation starting from early systole, peak systole and diastole, respectively.

4.1. Wall Shear Stress(WSS) distribution

WSS is an important factor to determine the effect of severity of arterial stenosis. It depends on the viscosity of the fluid and velocity gradient and, is defined as $\tau = \mu \frac{du}{dr}$, where μ is the viscosity and $\frac{du}{dr}$ is the velocity gradient.

Figures, 4(a), 4(b), 4(c) show the contours of WSS in normal carotid artery and 75% (by area) stenosed carotid artery and Figs.5(a), 5(b), 5(c) show the comparisons of WSS in both stenotic artery at early-systole, peak systole and diastole respectively. In both cases, WSS is uniformly distributed at CCA regions. The results reveal that the flow pattern changes abruptly in the region of stenosis throat and bifurcation onwards in the downstream whereas no significant change is observed in the upstream and it is significantly observed that the changes of WSS is due to stenosis and bifurcation. Surprisingly a sharp raise of WSS and immediately decline are observed in the stenotic throat. From the comparisons, our finding is that maximum WSS is observed at peak systole due to stenosis. After bifurcation WSS becomes high due to stnosis at all cases and then WSS becomes more low at peak systole and diastole.

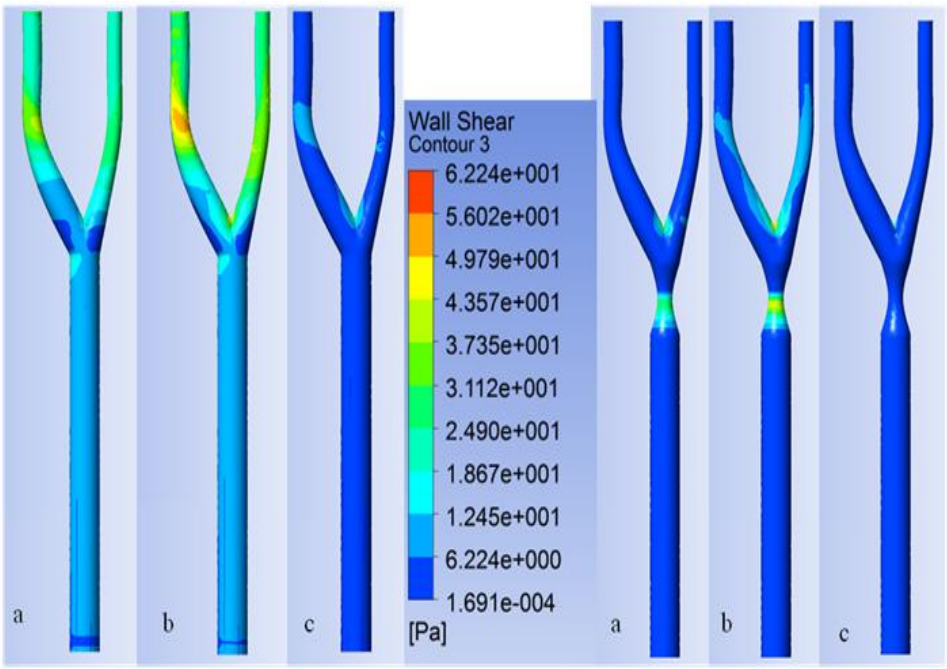

Figure 4:Comparison between Carotid artery and Stenosed carotid artery WSS contour at (a) early systole (b) peak systole and (c) diastole.

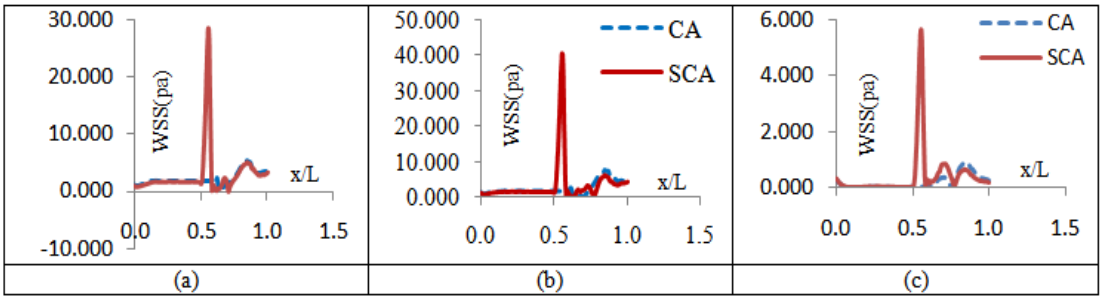

Figure 5:Comparison between Carotid artery and Stenosed carotid artery WSS distribution at (a) early systole (b) peak systole (c) diastole.

4.2.Velocity distribution

In figure 6, inlet velocity in both geometries begins with same magnitude for all case. Velocities at the throat and post stenotic region for all cases of SCA are relatively higher than that of CA according artery. Recirculation region is observed in SCA at post stenotic region for all cases. In the other hand, velocity is laminar in CCA region for all cases. The highest velocity is observed in SCA at peak systole and the lowest velocity is observed in CA at diastole.

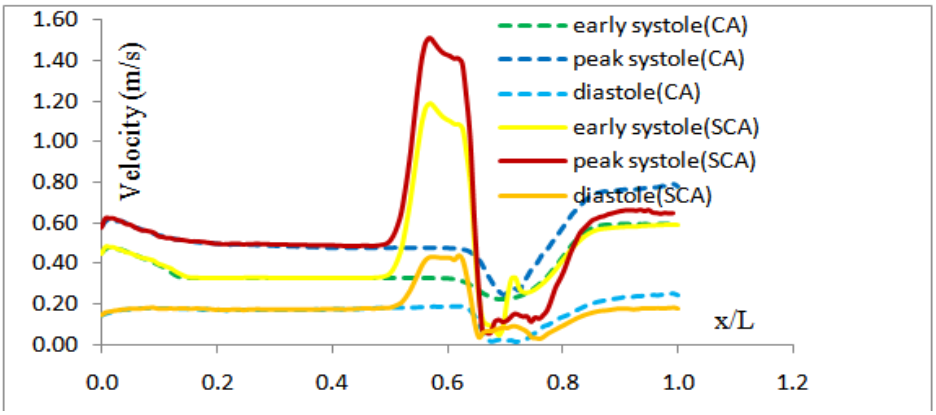

Figure 6: Comparison between Carotid artery and Stenosed carotid artery at different pulse cycle.

Comparison between Carotid artery and Stenosed carotid artery velocity contours at cross-section (a) early systole (b) peak systole and (c) diastole at distance from velocity-inlet (i) 0.0mm (VI) ,(j) 0.072mm, (k) 0.08mm (middle of stenosis), (l) 0.088mm (bifurcation point) and (m) 0.103mm are shown in figure 4.4.. In all cases we see no change in velocity distribution before stenotic region. Figure 4.4 shows due to bifurcation velocity decreases in all cases and velocity is higher in inner side than the outer side of the artery. The presence of stenosis increases the phenomena,so the possibility of formation plaque in outer wall is high.

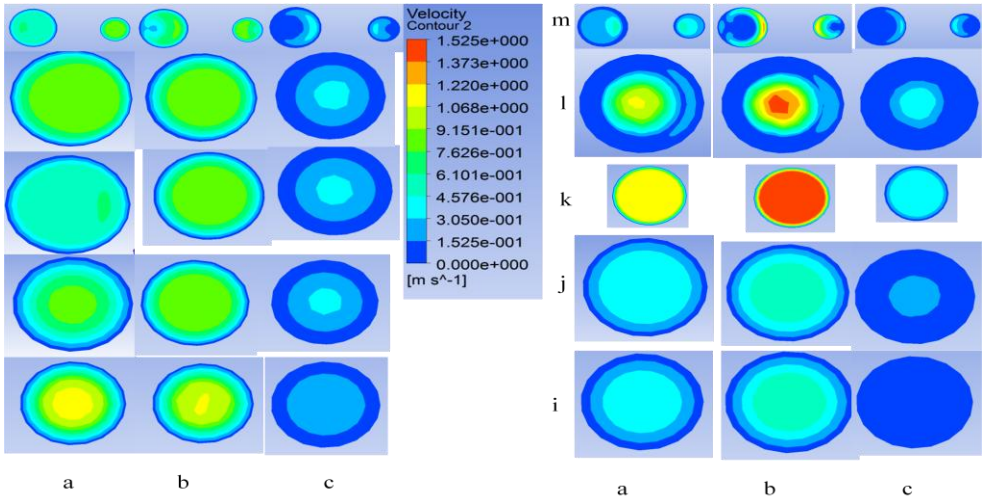

Carotid Artery Stenosed Carotid Artery

Figure 7:Comparison between Carotid artery and Stenosed carotid artery velocity contour at cross-section (a) early systole (b) peak systole and (c) diastole at distance from velocity-inlet (i) 0.0mm (VI) ,(j) 0.072mm, (k) 0.08mm (middle of stenosis), (l) 0.088mm (bifurcation point) and (m) 0.103mm .

4.3. Pressure distributions

Pressure contour in both arteries at early-systole, peak-systole, and diastole are shown in Figure 8 and cross-sectional pressure distribution along diameter are shown in figure 9. Figure 8(a) shows the contour of pressure in CA and SCA at early-systole. In CA the pressure is uniform and is varying with a small variation throughout the geometry. High pressure at pre-stenotic region and sudden decline of the pressure at the throat are characterized in SCA. Again, figure table 1 show that the pressure at middle point of cross-section (j), (k) (l), (m) and (n) for CA and SCA are as follows:

		(j) mmHg	(k) mmHg	(l) mmHg	(m) mmHg	(n) mmHg
Early systole	CA	102.31	102.2	102.2	99.90	99.93
	SCA	105.76	100.83	101.17	99.85	99.96
Peak systole	CA	102.53	102.53	102.53	102.39	102.30
	SCA	108.23	100.13	100.88	100.92	102.31
Diastole	CA	99.80	99.84	99.87	102.09	101.94
	SCA	100.17	99.73	99.82	101.72	102.47

Table 1: Pressure at middle point of different cross-section

The results clearly noticed that SCA can cause fatal death by blasting the pre stenotic arterial region of the patient of high blood pressure. From figure 8(c), we observe that, pressure is uniform and changing with a small variation before the throat. From table 1, it is observed that, the pressure at before throat and throat for CA are 99.80 mmHg and 99.84 mmHg and for SCA are 100.17 mmHg and 99.73 mmHg respectively. It is well known that pressure difference may provide some kind of extra force that may drive blood through the stenosis with high velocity. Since The pressure difference in SCA is higher than that of CA for all case. So at every case SCA creates more force than CA at their pre-stenotic region.

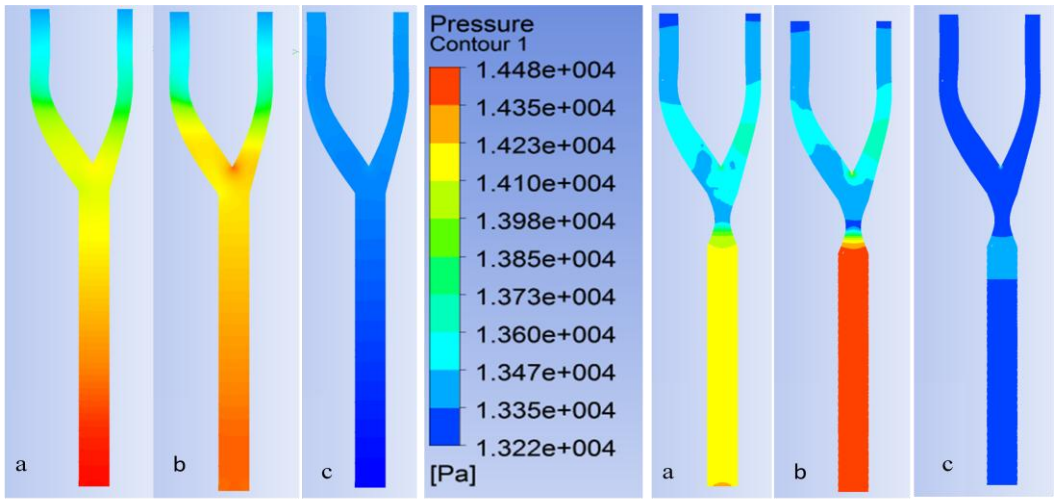

Figure 8: Comparison between Carotid artery and Stenosed carotid artery pressure contour at (a) early systole (b) peak systole and (c) diastole.

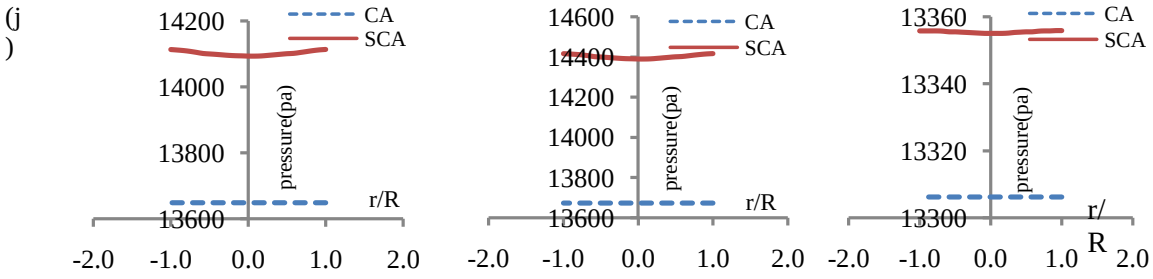

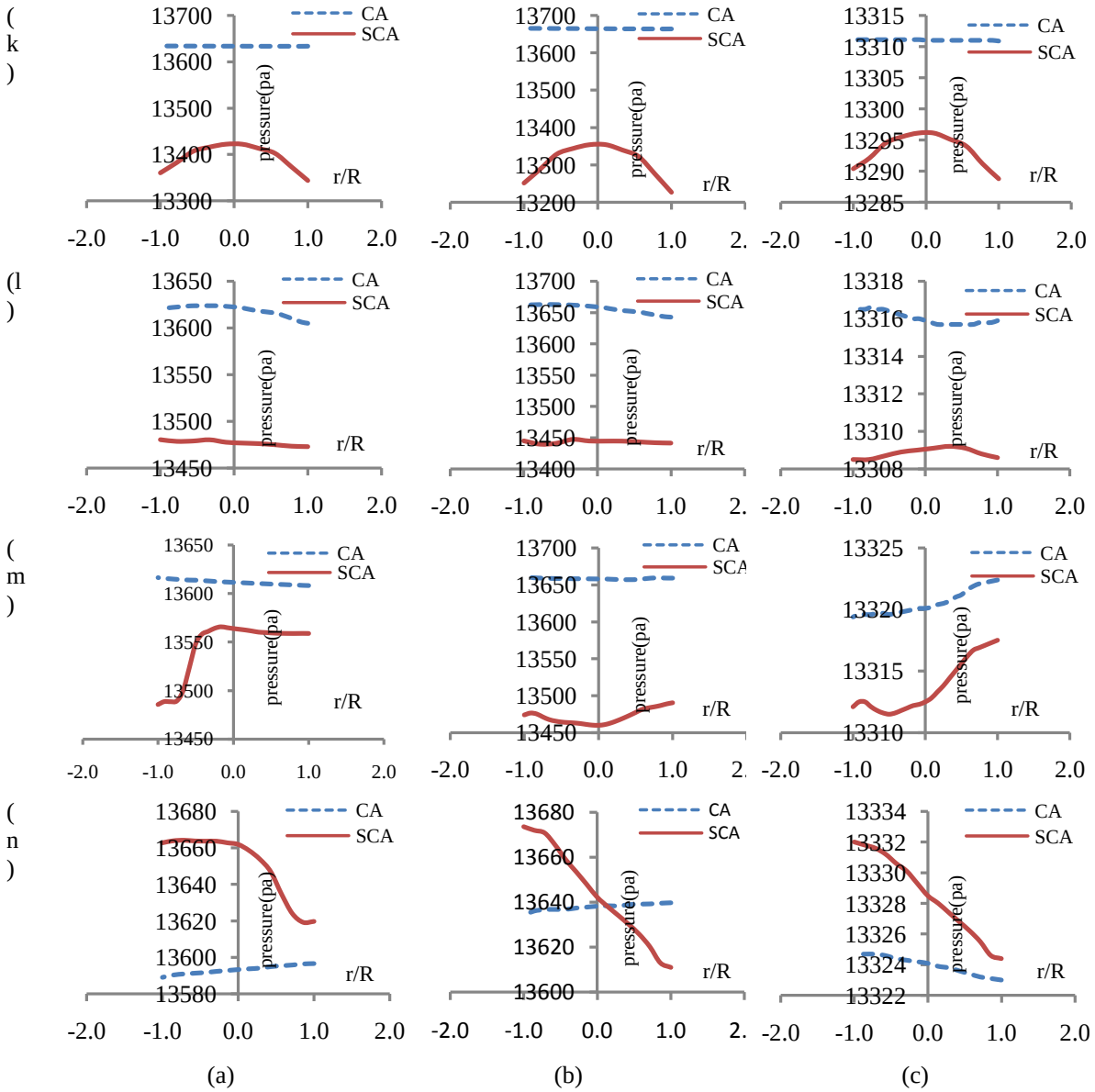

Figure 9: Comparison between Carotid artery and Stenosed carotid artery pressure distribution at cross-section along diameter (a) early systole (b) peak systole and (c) diastole at distance from velocity-inlet (j) 0.072mm, (k) 0.08mm (middle of stenosis), (l) 0.088mm (bifurcation point), (m) 0.103mm(ICA) and (n) 0.103(ECA).

4.4Streamline contours

Variations of streamlines contours have been investigated for CA and SCA to study the flow pattern of blood through artery. Streamline distribution for the models at early-systole, peak-systole, and diastole is shown in figure10. At early systole there is no vortex in CA and streamlines run smoothly throughout the geometries. But in SCA a very small vortex is noticed after the throat and bifurcation region, except this most of the streamlines run smoothly throughout the geometry. At peak all arteries create vortex. Two large vortexes at the post stenotic region near the throat are seen in SCA and a little turbulence is seen at ICA in CA. But there are differences in vortex size and shape. At diastole all arteries create significant size of vortex. Length of vortex is increased in SCA. Significant streamline differences are observed among the arteries. SCA create large difference in streamline from CA.

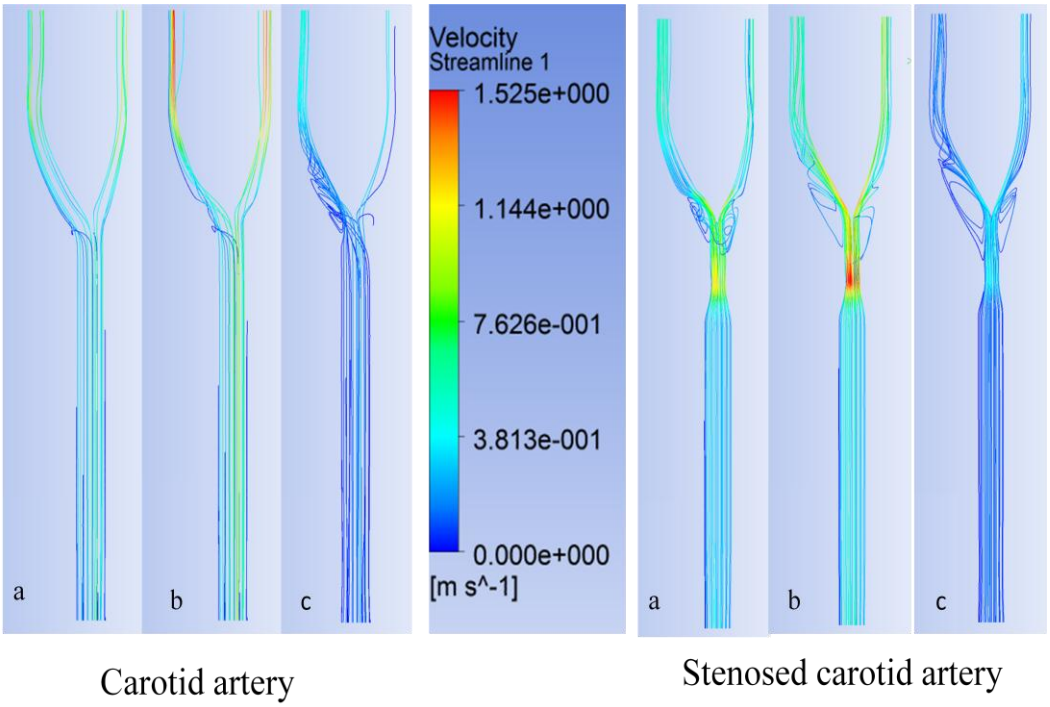

Figure 10: Comparison between Carotid artery and Stenosed carotid artery velocity streamline at (a) early systole (b) peak systole and (c) diastole.

V. Conclusion

Numerical simulations are performed on pulsatile blood flow through carotid artery and 75% severity stenosed carotid artery. Sinusoidal velocity profiles are imposed at inlet for the simulations. Wall shear stress distribution shows that as severity increases, shearing of flow also increases for all cases. And maximum stress is exerted in throat region at peak systole. Pressure distribution demonstrate that at every case stenosed carotid artery creates more force than normal carotid artery at their pre-stenotic region and 75% arterial stenosis can cause fatal death by blasting the pre stenotic arterial region of the patient of high blood pressure. Due to stenotic constriction, the flow behavior changes abruptly in the downstream of the stenosis. During peak systole the flow increases at the throat region forming a jet and later disrupts suddenly forming eddies due to pressure drop in downstream side. Analysis of streamline shows that a recirculation region is visible at the post stenotic region at 75% stenotic carotid artery for all cases and recirculation region increases with increasing minimum velocity at the inlet flow. Finally, significant flow changes are noticed in stenosed carotid artery. So stenosis is very harmful condition to any patient.

References

[1]. Lopez AD, Mathers CD, Ezzati M, Jamison DT and Murray CJ., "Global and regional burden of disease and risk factors, 2001:systematic analysis of population health data", Lancet 367:1747-1757, (2006).
[2]. Lloyd-Jones D, Adams RJ, Brown TM, Carnethon M, Dai S, et al., "Heart disease and stroke statistics-2010 update: a report from the American Heart Association" Circulation 121:e46-e215, (2010).
[3]. Hankey GJ, Jamrozik K, Broadhurst RJ, Forbes S and Anderson CS., "Long-term disability after first-ever stroke and related prognostic factors in the Perth Community Stroke Study," 1989-1990. Stroke 33:1034-1040., (2002).
[4]. Mohan KM, Crichton SL, Grieve AP, Rudd AG, Wolfe CD, et al., "Frequency and predictors for the risk of stroke recurrence up to 10 years after stroke," the South London Stroke Register. J Neurol Neurosurg, Psychiatry 80:1012-1018. (2009).
[5]. Putaala J, Haapaniemi E, Metso AJ, Metso TM, Artto V, et al., "Recurrent ischemic events in young adults after first-ever ischemic stroke.," Ann Neurol 68:661-671., (2010).
[6]. O'Donnell MJ, Xavier D, Liu L, Zhang H, Chin SL, et al., "Riskfactors for ischaemic and intracerebral haemorrhagic stroke in 22 countries(the INTERSTROKE study): a case-control study.," Lancet 376:112-123., (2010).
[7]. S. Khader and B. Shenoy., "Effect of increased severity in patient specific stenosis,World journal of Modelling and Simulation", Vol. 7 No. 2,pp. 113-122,(2011).
[8]. M.X. Li, J.J. Beech-Brandt, L.R. John,P.R.Hoskins and W.J. Easson., "Numerical analysis of pulsatile blood flow and vessel wall mechanics in different degrees of stenosis",J. Biomech, 40, 3715-3724.,(2007).
[9]. C, Chua and G. Shread., "Changes in flow and wall stresses through arterial constriction offset from the centre of the vessel", The Anziam Journal, 50: C744-C759,(2009).
[10]. August, A.D., B. Ariff, S. A. G. McG. Thom, X.Y. Xu and A. D. Hughes., "Analysis of complex flow and relationship between blood pressure, wall shear stress and intima-media thickness in the humen carotid artery",Am. J. physiol . Heart Cir. Physiol.293:1031-1037,(2007).
[11]. Bale-Glickman, J.K. Selby, D. Saloner and O. Savas., "Experimental flow studies in exact-replica phantoms of atherosclerotic carotid bifurcationsunder steady input conditions", J. Biomech. Eng. 125(1):38-48,(2003).

[12]. Kohler, U. I. Marshall, M.B. Robertson, Q. Long and X. Y. Xu., "MRI measurement of wall shear stress vectors in bifurcation models and comparison with CFD predictions", J. magn. Reson. Imaging 14(5): 563-573,(2001).
[13]. Fischer, P. F., F. Loth, S. E. Lee, S.W. Lee, D. Smith and H. Bassiouny., : "Simulation of high Reynolds number vascular flows",Comput. Methods Appl. Mech. Eng. 196: 3049-3060,(2007).
[14]. Steinman, D.A., T.L. Poepping, M. Tambasco, R. N. Rankin and D. W. Holdsworth., "Flow patterns at the stenosed carotid bifurcation: effect of concentric versus eccentric stenosis", Ann. Biomed. Eng. 28(4):415-423,(2000).
[15]. Stroud, J. S. A. Berger and D. Saloner., "Numerical analysis of flow through a severely stenotic carotid artery bifurcation", J. Biomech. Eng.124:9-20,(2002).
[16]. S. Lee and S. Lee., "Direct numerical simulation of transitional flow in a stenose carotid bifurcation", Journal of Biomechanics,41:2551-2561,(2008).
[17]. V. Young, A. Patterson M. Graves, Z-Y LI, V. Tavani, T. Tang, and J. H. Gillard, The British Journal of Radiology, S39-S45 (2009).
[18]. J. Pinto, K.L. Bessa, D.F. Legendre, and R.H. Prado, ABCM Symposium in Bioengineering, vol. 01, 2006.
[19]. S.A. Ahmed, and D.P. Giddens, Journal of Biomechanics, 17, 695-705 (1984).
[20]. G. Lorenzini, and E. Casalena, Journal of Biomechanics, 41, 1862–1870 (2008).
[21]. K Mamun, M.N.Akhter, M.S.H.Mollah,M.A.N.Sheikh, and M.Ali, The 6th BSME International Conference on Thermal Engineering, Dhaka(2014), edited by A.K.M. Sadrul Islam, M. Ruhul Amin, Mohammad Ali and Toshiaki Setoguchi (Procedia Engineering, 2015), vol. 150, pp. 877-884.
[22]. S.S. Varghese and S.H. Frankel, Journal of Biomechanics, 125, 445-460 (2003).

Mohammad Matiur Rahman Comparative Study of Netonian Sinusoidal Blood Flow through Normal and Stenosed Carotid Artery. IOSR Journal of Mathematics (IOSR-JM) , vol. 13, no. 6, 2017, pp. 08-17.